



# Hydrogen in polar intermetallics: Syntheses and structures of the ternary $\text{Ca}_5\text{Bi}_3\text{D}_{0.93}$ , $\text{Yb}_5\text{Bi}_3\text{H}_x$ , and $\text{Sm}_5\text{Bi}_3\text{H}_{\sim 1}$ by powder neutron or single crystal X-ray diffraction

E. Alejandro Leon-Escamilla<sup>a</sup>, Panagiotis Dervenagas<sup>b</sup>, Constantine Stassis<sup>b</sup>, John D. Corbett<sup>a,\*</sup>

<sup>a</sup> Department of Chemistry and Ames Laboratory-DOE, Iowa State University, Ames, IA 50011, USA

<sup>b</sup> Department of Physics and Ames Laboratory-DOE, Iowa State University, Ames, IA 50011, USA

## ARTICLE INFO

### Article history:

Received 16 July 2009

Received in revised form

15 October 2009

Accepted 25 October 2009

Available online 3 November 2009

### Keywords:

Interstitial atoms

Diffraction

Impurities

Hydride

## ABSTRACT

The syntheses of the title compounds are described in detail. Structural characterizations from refinements of single crystal X-ray diffraction data for  $\text{Yb}_5\text{Bi}_3\text{H}_x$  and  $\text{Sm}_5\text{Bi}_3\text{H}_{\sim 1}$  and of powder neutron diffraction data for  $\text{Ca}_5\text{Bi}_3\text{D}_{0.93(3)}$  are reported. These confirm that all three crystallize with the heavy atom structure type of  $\beta\text{-Yb}_5\text{Sb}_3$ , and the third gives the first proof that the deuterium lies in the center of nominal calcium tetrahedra, isostructural with the  $\text{Ca}_5\text{Sb}_3\text{F}$ -type structure. These Ca and Yb phases are particularly stable with respect to dissociation to  $\text{Mn}_5\text{Si}_3$ -type product plus  $\text{H}_2$ . Some contradictions in the literature regarding  $\text{Yb}_5\text{Sb}_3$  and  $\text{Yb}_5\text{Sb}_3\text{H}_x$  phases are considered in terms of adventitious hydrogen impurities that are generated during reactions in fused silica containers at elevated temperatures.

© 2009 Elsevier Inc. All rights reserved.

## 1. Introduction

Polar intermetallic compounds have been the focus of research for many scientific groups worldwide. Some of the interest in these lies in the cornucopia of structures and compositions that can often be rationalized in terms of the simple yet effective Zintl–Klemm principles [1]. But such studies are not without diversions and complications. A new phase that may be found in an otherwise well-studied binary system that cannot be reproduced in high yield suggests involvement of a third element or an otherwise uncontrolled variable. Such an additional element is normally bound either as an interstitial ion or through fractional substitution on a main atom site.

Of some importance for us have been the families of compounds with  $A_5B_3$ -type compositions that are formed between alkaline-earth or divalent rare-earth metals and tetragens (group 14) or pnictogens (15) [2–5]. Complications arose when it was discovered that interstitial hydrogen may play a major role in the formation of certain structure types among these. Historically, the hydrogen in these systems occurred primarily as an impurity, apparently either from (1) the active metal or (2) water desorbed from fused silica containers during high temperature syntheses or annealing processes. Its presence can naturally remain unnoticed

when characterization by X-ray diffraction prevails unless the structure type is characteristic of only the ternary hydride.

Regarding suspicions about unrecognized hydrogen components, neutron diffraction and direct chemical analyses would be the studies of choice, but their availability is limited. Alternatively, the presence of hydride in a compound can be indirectly demonstrated in some cases through careful and well-controlled experiments. For instance, dissociative reactions at high temperatures to give other products along with variations in the lattice parameters of the former can be indicative of hydride solutions. Reactions that substitute fluoride for hydride can be useful in some cases as well, but the chemistries of hydride versus fluoride may not be similar for the more metallic rather than salt-like phases.

Before our work on  $A_5Pn_3$  phases ( $A = \text{Ca–Ba, Sm, Eu, Yb}$ ;  $Pn = \text{Sb, Bi}$ ), no general structural trends for these so-called binaries seemed evident [2,3]. Some were reported in the hexagonal  $\text{Mn}_5\text{Si}_3$ -type structure ( $M$  hereafter), others as the orthorhombic  $\beta\text{-Yb}_5\text{Sb}_3$ -type ( $Y$ ), and a few in both types. Careful work with freshly dehydrogenated metals, control experiments with the binary hydride  $AH_x$  reactants, and development of reaction procedures under continuous high vacuum resolved the problems indirectly. All previously reported cases of  $A_5Pn_3$  compounds with divalent cations in  $Y$ -type structures were in fact hydrogen-stabilized compounds. These conclusions were reinforced when the equivalent fluoride-containing phases  $A_5Pn_3F$  could be prepared, for which classification in terms of the first example

\* Corresponding author. Fax: +1 515 294 6789.

E-mail address: [jcorbett@iastate.edu](mailto:jcorbett@iastate.edu) (J.D. Corbett).

$\text{Ca}_5\text{Sb}_3\text{F}$  as *F*-type [6] is more appropriate for a true ternary phase. However, verification that the H (D) atoms in the stuffed *Y*-type products are indeed in the same interstitial site as in  $\text{Ca}_5\text{Sb}_3\text{F}$  has not been accomplished before. In addition, such impurity generalizations among apparent stuffed *Y*-(or *F*-) type structures that contain divalent cations have recently been shown not to apply for some trivalent rare-earth-metal antimonides. The exceptional  $\text{Er}_5\text{Sb}_3$  and  $\text{Tm}_5\text{Sb}_3$  are instead stable in the  $\beta\text{-Yb}_5\text{Sb}_3$ -type (*Y*) structure at high temperatures [7].

We disclose here some specific details about the syntheses of  $\text{Ca}_5\text{Bi}_3(\text{H,D})_x$ ,  $\text{Yb}_5\text{Bi}_3\text{H}_x$  and  $\text{Sm}_5\text{Bi}_3\text{H}_x$ , all *F*-type according to X-ray diffraction. In addition, the refined crystal structures of  $\text{Ca}_5\text{Bi}_3\text{D}_x$  from powder neutron diffraction data and of the heavier atoms in the Yb and Sm hydride analogues from single crystal X-ray diffraction studies are described. The disputed dimorphism of  $\text{Yb}_5\text{Bi}_3(\text{H}_x)$  [2,3,8] is considered as well.

## 2. Experimental section

**Syntheses:** The elements utilized were Ca from APL Engineering (Alfa-Aesar), distilled and sealed in glass, Sm and Yb, Ames Laboratory (> 99.99% total, as received), and Bi, ORNL reactor grade. The  $\text{D}_2$  and  $\text{H}_2$  reactants were from Matheson, 99.5% and 99.999%, respectively. The binary Ca, Yb and Sm hydrides were prepared by direct reaction of  $\text{H}_2$  with heated metals held in a Mo boat within a vacuum system equipped with a diaphragm manometer [5]. The  $(\text{Ca,Yb})\text{H}_2$  phases were treated as stoichiometric and the third, as hexagonal  $\text{SmH}_{\geq 2.5}$  according to the respective cell dimensions. All reagents and products were handled in glove boxes with 0.2–0.4 ppm (vol)  $\text{H}_2\text{O}$  levels.

The dehydrogenation (cleaning) of the starting metals and the preparations of intermetallic compounds were done according to established procedures [2–5]. Dehydrogenations of Ca and Yb sealed in Ta containers were accomplished in a fused silica portion of a high-vacuum system ( $\leq 10^{-5}$  torr by heating them at 650 and 710 °C, respectively, for ~12 h or until the vacuum fell below that giving a Tesla coil discharge. This is effective because Ta becomes relatively transparent to hydrogen above ~550 °C. The same process was used to ‘clean’ binary pnictides. The *F*-type  $\text{A}_5\text{Bi}_3\text{H}_x$  samples,  $A=\text{Ca, Yb}$ , came from reactions between the elements with or without metal hydrides that had been sealed inside Ta containers and in turn heated within evacuated, well-flamed and sealed silica jackets. Each composition in Ta was encapsulated inside a separate  $\text{SiO}_2$  jacket in order to minimize hydrogen contributions from other sources. It is important to note that the fused  $\text{SiO}_2$  jackets afford some hydrogen values (plus an  $\text{R}_2\text{O}_3$  side-product) in the presence of R because of dehydration of the silica, faster at higher temperatures. The effect of this is critically dependent on the system and the relative stabilities of any relatively hydrogen-poorer *M*-type  $\text{A}_5\text{Bi}_3\text{H}_y$  phases that may be in equilibrium, the last appearing to be particularly low in hydrogen for the Ca and Yb products [3]. The binding and relative amounts of hydrogen in our samples were deduced from the variations in their structure types and, for *F*-type phases, from their lattice dimension variations with hydrogen content. Single phase products with *Y*-(not *M*-) type structures with hydrogen impurities were generally obtained from all pseudo-binary reactions run in sealed silica enclosures.

**Preparation of  $\text{Ca}_5\text{Bi}_3\text{D}$ :** Monophasic  $\text{Ca}_5\text{Bi}_3\text{D}$  was prepared by a two-step procedure in a high-vacuum hydrogenation system provided with gas buffer zones and a diaphragm manometer. Dehydrogenation of ~5.00 g of (Ca + Bi) was accomplished as above but at 1100 °C for 1 h, after which dried  $\text{D}_2$  gas was slowly introduced to ~400 torr and maintained at this pressure for the rest of the experiment. The reaction sequence was 2 h at 1100 °C,

72 h at 850 °C, further slow cooling to 650 °C, and then cooling to RT. The material close to the walls of the Ta container was not included in the diffraction sample although there was no direct evidence for any impurities.

All reactions, their conditions, products and the lattice constants for the *F*-type phases as well as some data from the literature are summarized in Table 1 for later discussion.

**Neutron diffraction analysis:** Neutron diffraction data were collected in the high-resolution powder diffractometer HB-4 at the Oak Ridge National Laboratory Neutron Facility. The neutron beam, generated by the decay of highly enriched  $^{235}\text{U}$ , was monochromatized by the (115) reflection from a Ge crystal that provided a wavelength of 1.4177 Å. A bank of 32 equally-spaced  $^3\text{He}$  detectors covered  $11 \leq 2\theta \leq 135^\circ$ . Data from ~2.8 g of  $\text{Ca}_5\text{Bi}_3\text{D}$  sealed in an In-gasketed V metal can were collected at room temperature over ca. 20 h. The GSAS34 software package was used to process and refine the data by least-squares means [9]. The atom positions reported for  $\text{Ca}_5\text{Bi}_3\text{F}$  [6] were the starting point for the refinement, and these were sequentially freed until no shift was observed. General collection data, refined atom positions, and the Ca–D distances are given in Tables 2 and 3, respectively.

**X-ray diffraction characterizations:** Product identifications were made with the aid of an EN FR552 Guinier powder pattern camera and NIST Si as an internal standard ( $\lambda(\text{Cu-K}\alpha 1)=1.54056$  Å). The phase distributions were estimated therefrom in terms of equivalent X-ray scattering powers with the aid of the calculated patterns of known phases. Variations in lattice constants derived from least-squares refinements served to differentiate relative hydrogen contents among ternary hydrides, which showed the customary decrease with increased content.

Crystals of  $\text{Yb}_5\text{Bi}_3\text{H}_x$  and  $\text{Sm}_5\text{Bi}_3\text{H}_{\sim 1}$  were selected with the aid of low magnification microscopy and were mounted in thin-walled glass capillaries within a nitrogen-filled glove box. Their quality was checked first with the aid of Laue photographs. Data were collected at room temperature on a Rigaku AFC6R diffractometer instrument ( $\omega$ – $2\theta$  scans) and monochromatized  $\text{MoK}\alpha$  radiation. Absorption was corrected with the aid of three psi-scans collected at  $\chi \geq 80^\circ$  and, after isotropic refinement, with DIFABS [10]. Converged structural refinements (on *F*) with 44 variables and a secondary extinction correction with the aid of the TEXSAN package [11] for  $I/\sigma(I) \geq 3$  data served mainly to confirm the basic heavy atom structures and to establish their dimensions. (The  $F_o/F_c$  listings are available from J.D.C.) Lattice dimensions secured by least-squares refinement of calibrated Guinier powder pattern data were used in all distance calculations from single crystal data. Refinements of heavy atom occupancies gave no indications of any significant deviation from the 5:3 stoichiometries. Some general data collection parameters are in Table 4, the refined atom positions and isotropic-equivalent displacements are in Table 5, and the corresponding anisotropic displacement data are contained in Supplementary Material.

## 3. Results and discussion

Among the  $\text{A}_5\text{Pn}_3\text{H}_x$  phases, the Ca–Bi and Yb–Bi combinations have been shown to have the strongest hydrogen binding and greatest tendency to transform from the normal (binary) *M*-type materials into the stuffed  $\beta\text{-Yb}_5\text{Sb}_3$  ( $\text{Ca}_5\text{Sb}_3\text{F}$ -type) phases, even for quite low hydrogen activities [3]. One important indicator for this is the size ratio between ions. The Ca and Yb bismuthides show the smallest *A*:*Pn* size proportions among all known members of the  $\text{A}_5\text{Pn}_3\text{H}_x$  family, and therefore contain the smallest *A* atom tetrahedra as nearest neighbors of the hydride, whereas lattice energy stability terms vary as the *sum* of the two radii and would be least for bismuth. The effect is so great that these two 5:3 hydrides have appeared to be

**Table 1**  
Synthetic reactions for (Ca,Yb,Sm)<sub>5</sub>Bi<sub>3</sub>H phases and lattice parameters of F-type products (Å).

No.	Loaded compositions	Reaction conds. <sup>a</sup>	Structure types of main products <sup>b</sup>	Lattice dimensions (Å) (F-type) <sup>c</sup>			Vol	Ref
				a	b	c		
1	Ca <sub>5</sub> Bi <sub>3</sub>	i (dv)	95% F, ~5% M	12.7729(7)	9.6921(5)	8.4326(5)	1043.9(1)	[2,3]
2	Ca <sub>5</sub> Bi <sub>3</sub>	ii (dv)	90% M, ~8% F					[3]
3	Ca <sub>5</sub> Bi <sub>3</sub> (no.2)	iii (sc)	F	12.718(1)	9.6993(7)	8.4315(5)	1040.1(1)	
4	Ca <sub>5</sub> Bi <sub>3</sub> H <sub>0.0</sub>	iv (sc)	92% F, ~6% M	12.7602(7)	9.6924(5)	8.4330(4)	1042.97(9)	[2]
5	Ca <sub>5</sub> Bi <sub>3</sub> H <sub>0.5</sub>	iv (sc)	F	12.6972(7)	9.7036(5)	8.4334(4)	1039.06(9)	
6	Ca <sub>5</sub> Bi <sub>3</sub> H <sub>1.0</sub>	iv (sc)	F	12.609(1)	9.7141(8)	8.4443(7)	1034.3(2)	[2]
7	Ca <sub>5</sub> Bi <sub>3</sub> H <sub>2.0</sub>	iv (sc)	F	12.611(2)	9.714(1)	8.442(1)	1034.2(2)	
8	Ca <sub>5</sub> Bi <sub>3</sub> D <sub>x</sub>	v	F	12.608(1)	9.7078(9)	8.4398(8)	1033.0(1)	
9	Yb <sub>5</sub> Bi <sub>3</sub>	i (dv)	25% M, 75% F	–	–	–	–	[3]
10	Yb <sub>5</sub> Bi <sub>3</sub>	ii (dv)	85% M, 15% F	–	–	–	–	
11	Yb <sub>5</sub> Bi <sub>3</sub> (no. 10)	iii (sc)	F	12.638(4)	9.722(2)	8.407(2)	1033.0(5)	[2]
12	Yb <sub>5</sub> Bi <sub>3</sub> H <sub>0.0</sub>	iv (sc)	90% F, ~7% M	12.660(2)	9.714(1)	8.4067(6)	1033.9(2)	[2]
13	Yb <sub>5</sub> Bi <sub>3</sub> H <sub>0.5</sub>	iv (sc)	F	12.592(3)	9.730(2)	8.409(1)	1030.2(4)	
14	Yb <sub>5</sub> Bi <sub>3</sub> H <sub>1.0</sub>	iv (sc)	F	12.560(1)	9.7369(6)	8.4104(4)	1028.5(1)	[2]
15	Yb <sub>5</sub> Bi <sub>3</sub> H <sub>2.0</sub>	iv (sc)	F	12.459(5)	9.737(2)	8.414(2)	1028.1(2)	
16	Yb <sub>5</sub> Bi <sub>3</sub>	vi (dv)	F	12.6375(6)	9.7243(4)	8.4117(5)	1033.72(9)	[8]
17	Yb <sub>5</sub> Bi <sub>3</sub> H <sub>0.25</sub>	vii (sc)	F	12.6113(5)	9.7317(4)	8.4124(3)	1032.45(7)	[8]
18	Sm <sub>5</sub> Bi <sub>3</sub>	viii (dv)	30% M, 65% ATP	–	–	–	–	[3]
19	Sm <sub>5</sub> Bi <sub>3</sub> H <sub>2.0</sub>	ix (sc)	95% F, 5% ATP	13.1252(8)	10.1418(6)	8.7613(5)	1166.2(1)	[2]

<sup>a</sup> Reaction conditions: dv: dynamic high vacuum; sc: in sealed silica jacket. (i) dv conds: 1100 °C, 2 h, 10 °C/h to 650 °C, 50 °C/h to R.T. (ii) dv conds: 1100 °C, 18 h (induction heating), quench with N<sub>2</sub> (g) to R.T. (iii) sc conds: 850 °C, 26 days, quench to RT in ice. (iv) sc conds: 1100 °C, 3 h, 10 °C/h to 650 °C, 50 °C/h to R.T. (v) See experimental section. (vi) (a) dv conds: 1100 °C, 12 h; (b) sc conds: 1100 °C, 2 h, 8.3 °C/h to 900 °C, hold 7 days; quench to R.T. (vii) sc conds: same as vi-b. (viii) dv conds: 1150 °C 1 h, 50 °C/h to 1100 °C, hold 1 h; 10 °C/h to 650 °C, 50 °C/h to R.T. (ix) sc conds: 1150 °C, 1 h, 50 °C/h to 1100 °C; 10 °C/h to 650 °C; 50 °C/h to R.T.

<sup>b</sup> Structure types; F=Ca<sub>5</sub>Sb<sub>3</sub>F; M=Mn<sub>5</sub>Si<sub>3</sub>, ATP=anti-Th.

<sup>c</sup> Lattice parameters from Guinier powder patterns.

**Table 2**  
Data collection and refinement parameters from neutron diffraction by orthorhombic Ca<sub>5</sub>Bi<sub>3</sub>D (*Pmna*, No. 62, Z=4).

Compound	Ca <sub>5</sub> Bi <sub>3</sub> D <sub>0.93(3)</sub>
Lattice parameters (Å)	
a	12.6068(4)
b	9.7070(3)
c	8.4384(2)
Volume (Å <sup>3</sup> )	1032.65(4)
Density calc. (g/cm <sup>3</sup> )	5.334
Temperature (K)	298
Refined 2θ Region (°)	11–135
Total number of channels/reflections	2474/1597
Number of refined variables	31
R <sub>p</sub> (%)	5.37
R <sub>wp</sub> (%)	6.36
Reduced χ <sup>2</sup> (Goodness of Fit)	1.210
Final max. atom shift	0.00

**Table 3**  
Refined positional and displacement data and Ca–D distances (Å) from neutron diffraction on F-Ca<sub>5</sub>Bi<sub>3</sub>D.

Compound	Atom	x	y	z	10 <sup>2</sup> U <sub>iso</sub>
Ca <sub>5</sub> Bi <sub>3</sub> D	Ca1	0.0724(5)	0.0429(7)	0.1968(7)	1.4(2)
	Ca2	0.0099(7)	1/4	0.5337(9)	1.0(2)
	Ca3	0.2285(8)	1/4	0.821(1)	1.7(3)
	Ca4	0.2834(8)	1/4	0.3556(1)	1.1(2)
	Bi1	0.3294(3)	0.0178(3)	0.0722(5)	0.79(8)
	Bi2	0.4813(4)	1/4	0.5808(7)	0.81(1)
	D	0.1043(6)	1/4	0.3053(9)	1.2(3)
	Ca1–D	(2 ×)	2.245(8)		
Ca2–D		2.30(1)			
Ca3–D		2.27(1)			

pseudo-binary compounds under many synthetic conditions. The counterpart of this, the competing nominally binary M-type 5:3 phases in equilibrium take up the smallest amounts of hydrogen into

**Table 4**  
X-ray data collection and refinement results for orthorhombic (Yb,Sm)<sub>5</sub>Bi<sub>3</sub>H<sub>x</sub> (*Pmna*, No. 62, Z=4).

Compound	Yb <sub>5</sub> Bi <sub>3</sub> H <sub>x</sub>	Sm <sub>5</sub> Bi <sub>3</sub> H <sub>–1</sub>
Lattice parameters (Å) <sup>a</sup>		
a	12.660(2)	13.1252(8)
b	9.714(1)	10.1418(6)
c	8.4067(6)	8.7613(5)
Volume (Å <sup>3</sup> )	1033.9(2)	1166.2(1)
Density, calc. (g/cm <sup>3</sup> )	9.592	7.859
Octants collected	h, vk, l	h, vk, v l
Scan type	ω–2θ	ω–2θ
Relative transm. coeff. range	0.583–1.0	0.542–1.0
Absorption coeff. (cm <sup>–1</sup> )	953.0	697.7
No. reflections measured	2057	4378
indep. (obs., I > 3σ(I))	1079 (856)	1227 (776)
R <sub>ave</sub> (%)	9.26	8.70
Number of refined variables	44	44
R/R <sub>w</sub> (%)	4.3/5.4	2.7/3.0
Goodness of fit	1.849	1.363
Max./min. in ΔF map (e <sup>–</sup> · Å <sup>–3</sup> )	3.69/–3.12	2.04/–2.17

<sup>a</sup> Lattice parameters from Guinier powder pattern refinements.

oversized metal 'octahedra' before they transform to F-type ternaries, whereas the latter exhibit the widest ranges of hydrogen contents [3]. For these reasons, some additional information is presented here regarding the necessary synthetic precautions and the effects of various parameters for these particular examples.

**Synthesis and structure:** Ca<sub>5</sub>Bi<sub>3</sub>(H,D). Dynamic vacuum conditions that work well with almost all other A<sub>5</sub>Pn<sub>3</sub>–H systems when heated afford only about 5% of the hexagonal M-type Ca<sub>5</sub>Bi<sub>3</sub> phase, entry 1 in Table 1. Rather, evident residual hydrogen values in the high-vacuum system (including hydrocarbons) were sufficient during a relatively slow cooling process to generate the orthorhombic hydride. Thus it proved necessary to quench a sample under vacuum from 1100 °C, entry 2, in order to retain most of the hexagonal M-type phase. On the other hand, hydrogen that evidently originates from dehydration of the sealed silica

**Table 5**  
Positional and displacement parameters for  $\text{Yb}_5\text{Bi}_3\text{H}_x$  and  $\text{Sm}_5\text{Bi}_3\text{H}_{-1}$  from single crystal X-ray diffraction.

Compound	Atom	x	y	z	$B_{eq}(\text{\AA}^2)$
$\text{Yb}_5\text{Bi}_3\text{H}_x$	Yb1	0.07379(9)	0.0418(1)	0.1951(1)	0.99(4)
	Yb2	0.0058(1)	1/4	0.5338(1)	0.77(6)
	Yb3	0.2285(1)	1/4	0.8204(2)	0.85(6)
	Yb4	0.2876(1)	1/4	0.3501(2)	0.85(6)
	Bi1	0.32947(6)	0.01432(7)	0.06950(8)	0.67(3)
	Bi2	0.48334(8)	1/4	0.5791(1)	0.59(4)
$\text{Sm}_5\text{Bi}_3\text{H}_{-1}$	Sm1	0.0744(2)	0.0438(2)	0.1945(3)	0.87(7)
	Sm2	0.0051(3)	1/4	0.5344(4)	0.7(1)
	Sm3	0.2299(3)	1/4	0.8180(4)	0.8(1)
	Sm4	0.2900(3)	1/4	0.3476(4)	0.9(1)
	Bi1	0.3287(1)	0.0129(2)	0.0657(2)	0.59(7)
	Bi2	0.4834(2)	1/4	0.5797(3)	0.5(1)

jacket at 850 °C was also sufficient to convert most of a purified  $\text{Ca}_5\text{Bi}_3$  sample to the ternary hydride, even when quenched in ice, entry 3 (depending on proportions in the experiment, of course). The decrements in *M*-type cell volumes for both the Ca and Yb bismuthides are estimated to be only of the order of 0.05% before their transformations to the *F*-type products occur, compared with ~0.3% with Sr, for example. The much larger decrements in the cell volumes among the corresponding *F*-type products, Fig. 2, are consistent with their greater hydride contents, especially when the dynamic vacuum result is also included for  $\text{Ca}_5\text{Bi}_3\text{H}_x$  to allow for hydrogen background gained from silica contamination. The overall volume change is about 0.85%.

Confirmation of the H/D location and D content in  $\text{F-Ca}_5\text{Bi}_3\text{H}_{0.93(3)}$  by means of a neutron diffraction study seemed particularly important because of its extreme stability among the  $\text{A}_5\text{Pn}_3\text{H}_x$  phases. The synthesis result, entry 8, Table 1, was monophasic *F*-type with X-ray lattice parameters close to those of the hydrogen-saturated samples, and within two sigma of the slightly smaller values refined from neutron data, Table 2. Thus, refinement of the neutron diffraction data with only the heavy atom input for  $\text{Ca}_5\text{Bi}_3\text{F}$  [6] converged at  $R_p/R_{wp}$  residuals of 7.72/9.43 (%) and a reduced  $\chi^2$  of 2.7. But inclusion of D at the interstitial position of *F* led to convergence after full least-squares refinement of positions and a D occupancy of 5.37/6.36 and a reduced  $\chi^2$  of 1.2 for  $\text{Ca}_5\text{Bi}_3\text{D}_{0.93(3)}$ . (Of course, the occupancy result does not allow D and H to be distinguished.) These data and the Ca–D bonding distances are given in Tables 2 and 3, respectively, and the fitted diffraction histogram and the difference profile appear in Fig. 3.

The deuterium lies in a distorted tetrahedral cavity defined by the Ca1 ( $\times 2$ ), Ca2 and Ca4 with Ca–D distances from 2.24 to 2.30 Å ( $\sigma \sim 0.01$  Å,  $d_{ave} = 2.265$  Å), in good agreement with those anticipated from the 2.24 Å sum of crystal radius for  $\text{Ca}^{2+}$  (CN 6) and an empirical  $\text{H}^-$  radius of 1.10 Å [12]. The orthorhombic  $\text{Ca}_5\text{Bi}_3\text{D}$  structure (*Y*-type, *Pnma*,  $Z=4$ ) shown in a [010] view in Fig. 1 can be described in terms of very similar, but not superimposable, layers of Ca (black) at  $y = \frac{1}{4}$  and  $\frac{3}{4}$  that are related by glide planes normal to the *a*- and *c*- axes and by inversion through  $\frac{1}{2}, \frac{1}{2}, \frac{1}{2}$ . The Ca layers generate an infinite array of trigonal prisms along the view that also share two-thirds of their side edges. These are centered by Bi1 (white) atoms at  $y=0$  or  $\frac{1}{2}$ . This network also contains large hexagonal rings and, pairs of additional Ca1 and gray Bi2 atoms lie within the tunnels generated by the former. The Ca1 atoms together with one basal edge of the  $\text{Ca}_{6/2}(\text{Bi1})$  trigonal prisms define the important D-binding sites, a series of identical but separate and somewhat distorted Ca tetrahedral cavities (shaded) that run along *b*. The different shadings of their faces indicate that they lie at different depths, around  $b = \frac{1}{4}$  or  $\frac{3}{4}$ . Evidently, the numbers and sizes of the cavities, the elasticity of the structure, and the ideal presence of only one electron beyond a Zintl formulation for these hosts (with isolated Ca and Bi atoms) are

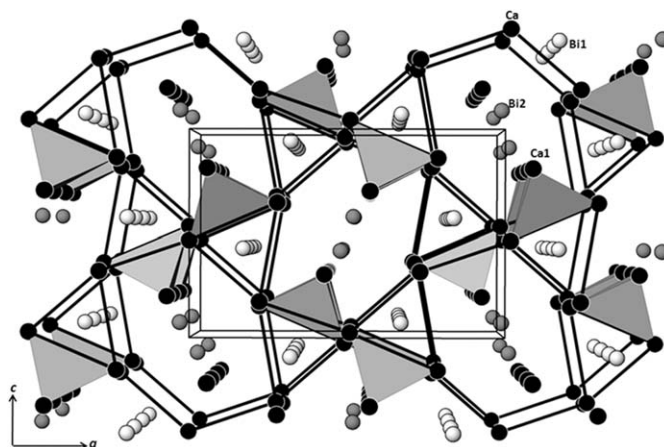


**Fig. 1.** [010] section of orthorhombic structure of  $\text{Ca}_5\text{Bi}_3\text{D}$  ( $\text{Ca}_5\text{Sb}_3\text{F}$ -type, *Pnma*,  $Z=4$ ). Black atoms are Ca and gray atoms are Bi1 or Bi2 (darker); all lie at or near  $b = \frac{1}{4}$  or  $\frac{3}{4}$ . The D atoms center the separate shaded  $\text{Ca}_4$  tetrahedra that lie at two different levels in the projection.

such that only a single F, H or D can be bound per formula unit, presumably with  $-1$  oxidation states. This interstitial result is in considerable contrast to the much more variable interstitial members possible in the large family of electron-rich stuffed  $\text{Mn}_5\text{Si}_3$ -type hosts in which trigonal antiprismatic cavities are filled [13]. Actually, there is a second exceedingly similar orthorhombic structure, entirely distinct from  $\beta\text{-Yb}_5\text{Sb}_3$ , that is commonly called the  $\text{Y}_5\text{Bi}_3$ -type in which both the *a* and *c* axial lengths and symmetry operations are reversed for the same space group setting. This member does not seem to take up interstitials in any of its examples [3]. The structural and theoretical relationships between these two types have recently been considered in connection with the truly binary  $\text{Er}_5\text{Sb}_3$  and  $\text{Tm}_5\text{Sb}_3$  examples, for which both orthorhombic structure types are found, the *Y*-( $\beta\text{-Yb}_5\text{Sb}_3$ -) type at higher temperatures [7].

$\text{Yb}_5\text{Bi}_3\text{H}_x$  and  $\text{Sm}_5\text{Bi}_3\text{H}_x$ : The orthorhombic  $\text{Yb}_5\text{Bi}_3\text{H}_x$  phase is second only to  $\text{Ca}_5\text{Bi}_3\text{H}$  in stability and dominance of the *F*-type form under ordinary synthesis conditions. Reactions leading to  $\text{Yb}_5\text{Bi}_3\text{H}_x$  gave very similar results and trends to those described for  $\text{Ca}_5\text{Bi}_3\text{H}_x$ , Table 1. Only small amounts of the pseudo-binary hexagonal *M*-type phase could be obtained following reactions under dynamic vacuum conditions or with a  $\text{Yb}_5\text{Bi}_3\text{H}_{0.0}$  loading run in sealed silica, entries 9 and 12, Table 1, respectively. A high yield of the *M*-type phase was obtained only after quenching from 1100 °C under active vacuum. Lattice dimensions of the products from  $\text{Yb}_5\text{Bi}_3\text{H}_{0.0-2.0}$  reactions follow the same trend as for the equivalent  $\text{Ca}_5\text{Bi}_3\text{H}_{0.0-2.0}$  products but with a cell volume decrement of ca. 0.56%, Fig. 2. X-ray crystal data for *Y*-type (heavy atom)  $\text{Yb}_5\text{Bi}_3\text{H}_x$  were collected from entry 12 reaction product that should have been at the lower hydrogen concentration limit in as much as the *M*-type phase was also present. The *F*-type crystal of  $\text{Sm}_5\text{Bi}_3\text{H}_x$  came from a  $\text{Sm}_5\text{Bi}_3\text{H}_{2.0}$  composition, entry 19. Under dynamic vacuum conditions, an equivalent reaction 18 yielded the *M*-type structure. The occurrence of the Sm-poorer, anti- $\text{Th}_3\text{P}_4$ -type co-product as well in 19 is not unusual for such a hydrogen-rich reaction; even in the case in which the product is close to saturation, i.e.,  $\text{Sm}_5\text{Bi}_3\text{H}_{-1}$ , some  $\text{SmH}_x$  presumably must remain as well, leading to a deficiency of Sm. Such a loading deficiency is evident for 18, Table 1.

A recent study of  $\text{Yb}_5\text{Bi}_3$  by Liang et al. [8] concluded that only the *Y*-type structure existed with or without hydride; that is, in samples with either a measured or no detectable hydrogen, and with an appropriate expansion of the cell for the latter. An *M*-type phase was never observed. However, they evidently failed to note two earlier studies that had proven both *Y*- and *M*-type phases

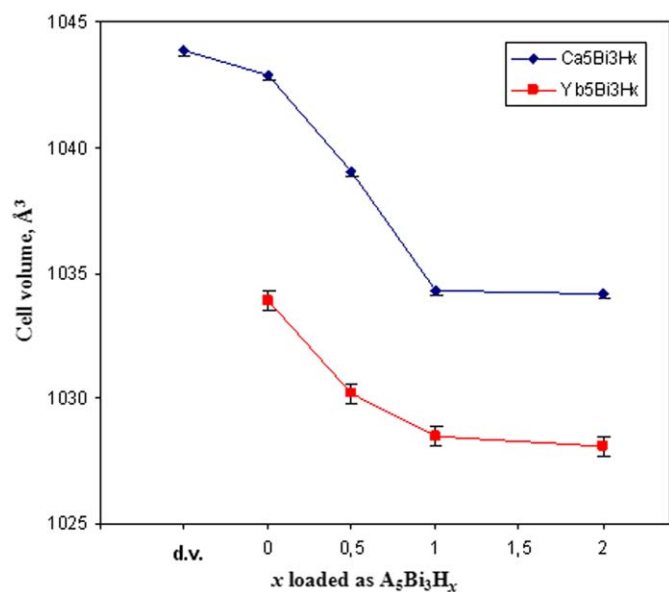


**Fig. 2.** Cell volumes of products of  $\text{Ca}_5\text{Bi}_3\text{H}_x$  and  $\text{Yb}_5\text{Bi}_3\text{H}_x$  reactions run in welded Ta containers within sealed  $\text{SiO}_2$  jackets as a function of loaded  $x$ . The marked  $d.v.$  point corresponds to entry 1 in Table 1, the lattice volume background for a binary reaction run in a sealed  $\text{SiO}_2$  jacket. (Error bars correspond to the largest standard deviation of the values on each curve).

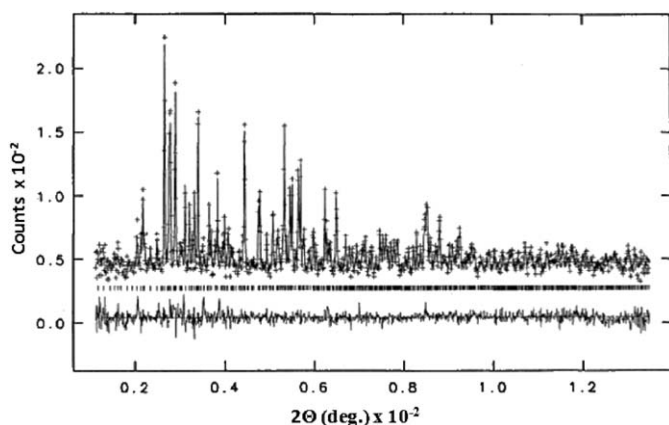


**Fig. 3.** Powder neutron diffraction histogram obtained for  $\text{Ca}_5\text{Bi}_3\text{D}$ . Lines and points represent the calculated and observed profile values, respectively, and the bottom curve, the difference between the other two.

were stable in the Yb–Bi system [2,3], the latter product only after taking particular precautions to eliminate hydrogen from the system (above). In fact their analytical detection limit for hydrogen,  $\sim 80$  ppm, corresponds to about  $\text{Yb}_5\text{Bi}_3\text{H}_{0.12}$ . This is very likely above the small amount required to stabilize the ternary Y structure, which produces a hexagonal cell volume expansion of the order of only 0.05% [3]. The lattice dimensions they reported for the supposed binary and ternary  $F$ -types,  $\text{Yb}_5\text{Bi}_3$  and  $\text{Yb}_5\text{Bi}_3\text{H}_{0.25}$  (items 16 and 17 in Table 1, respectively,) are in excellent agreement with (1) our entry 12, near the boundary for transformation of  $Y$ - to  $M$ -type and (2), by interpolation between entries 12 and 13 in Table 1, respectively. Note that their item 16 “ $\text{Yb}_5\text{Bi}_3$ ” sample also underwent a final annealing step in a closed silica container. Products of pseudo-binary reactions in the two bismuthide systems considered here that have been run in sealed silica containers *always* appear to be contaminated with and stabilized by hydride from that source. It is only the successful syntheses of the alternate  $\text{Mn}_5\text{Si}_3$ -type phases for  $\text{Ca}_5\text{Bi}_3$  and  $\text{Yb}_5\text{Bi}_3$  under more stringent conditions that make this clear [3].

**Table 6**

Interatomic distances ( $\text{\AA}$ ) in  $A_5\text{Pn}_3\text{H}_x$  phases ( $A=\text{Yb, Sm}$ ) with  $\text{Ca}_5\text{Sb}_3\text{F}$ -type structures.

Atom 1–Atom 2	$\text{Yb}_5\text{Bi}_3\text{H}_x$	$\text{Sm}_5\text{Bi}_3\text{H}_{\sim 1}$
A1–A1	3.869(5)	4.021(4)
A2–A1	(2 ×) 3.598(4)	3.751(3)
A2–A1	(2 ×) 3.789(3)	3.935(3)
A3–A2	(2 ×) 3.699(5)	3.850(4)
A3–A2	(2 ×) 3.712(5)	3.858(4)
A3–A1	(2 ×) 3.920(3)	4.081(3)
A3–A1	(2 ×) 4.231(4)	4.403(3)
A3–A4	4.027(5)	4.192(4)
A4–A1	(2 ×) 3.622(4)	3.766(3)
A4–A1	(2 ×) 4.135(4)	4.326(3)
A4–A1	(2 ×) 4.427(4)	4.604(3)
A4–A2	(2 ×) 3.934(5)	4.040(4)
A4–A2	4.210(5)	4.413(4)
Bi1–A1	3.398(3)	3.541(2)
Bi1–A1	3.410(3)	3.562(2)
Bi1–A1	3.719(3)	3.825(2)
Bi1–A2	3.317(3)	3.446(2)
Bi1–A2	3.319(3)	3.461(2)
Bi1–A3	3.348(3)	3.496(2)
Bi1–A3	3.402(3)	3.549(2)
Bi1–A4	3.341(3)	3.472(2)
Bi1–A4	3.485(3)	3.640(2)
Bi2–A1	(2 ×) 3.259(3)	3.413(2)
Bi2–A2	3.263(4)	3.406(3)
Bi2–A3	3.238(5)	3.345(3)
Bi2–A3	3.788(5)	3.950(3)
Bi2–A4	(2 ×) 3.103(3)	3.217(2)
Bi2–A4	3.126(5)	3.255(3)

Incidentally, the earliest report of  $M\text{-Yb}_5\text{Bi}_3$  [14] does not appear related to that recently described phase. Although the reported lattice type and dimensions were misreported, 13 of the 15 diffraction lines can be refined with hexagonal parameters:  $a=8.9881(4)$ ,  $c=6.9443(7)$   $\text{\AA}$ . Presuming their diffractometer calibration was satisfactory, these are about 0.20 and 0.10  $\text{\AA}$  less than values for the very slightly contracted  $\text{Yb}_5\text{Bi}_3$  ( $M$ ) in the presence of the orthorhombic  $F$ -phase, respectively [3]. Impurities of small second-period interstitials would be a reasonable cause of such differences, oxygen in particular [13].

Single crystal structures of these two compounds,  $\text{Yb}_5\text{Bi}_3\text{H}_x$  and  $\text{Sm}_5\text{Bi}_3\text{H}_{\sim 1}$ , do not reveal any unanticipated feature. Both refined smoothly starting with the heavy atom positions in the  $\text{Ca}_5\text{Sb}_3\text{F}$ -type. Table 6 contains a list of interatomic distances below 4.5  $\text{\AA}$ . Refinement of all heavy atom occupancies but for one cation site yielded  $\text{Yb}_{4.99(2)}\text{Bi}_{3.00(1)}$  and  $\text{Sm}_{4.98(2)}\text{Bi}_{3.00(1)}$  compositions. Interatomic distance comparisons for the orthorhombic  $\text{Yb}_5\text{Bi}_3\text{H}_x$  and  $\text{Sm}_5\text{Bi}_3\text{H}_{\sim 1}$  are both consistent with divalent rare-earth-metals, which can also be predicted from the cell volume ratio for  $F$ - versus  $M$ -forms, approximately 2.0:1, the ratio of formula units per cell for these two structure types. The cations in  $M$ -type  $\text{Sm}_5\text{Bi}_3$  are evidently trivalent [3].

### Supplementary material

Anisotropic displacement ellipsoid data for  $\text{Yb}_5\text{Bi}_3\text{H}_x$  and  $\text{Sm}_5\text{Bi}_3\text{H}_x$ .

### Acknowledgment

This research was supported by the Office of the Basic Energy Sciences, Materials Sciences Division, US Department of Energy (DOE). The Ames Laboratory is operated for DOE by Iowa State University under Contract no. AC02-07CH11358.

## Appendix A. Supplementary material

Supplementary data associated with this article can be found in the online version at doi:[10.1016/j.jssc.2009.10.024](https://doi.org/10.1016/j.jssc.2009.10.024).

## References

- [1] S.M. Kauzlarich (Ed.), Chemistry Structure and Bonding of Zintl Phases and Ions, VCH Publishers, New York, 1996.
- [2] E.A. Leon-Escamilla, J.D. Corbett, J. Alloys Compd. 265 (1998) 104.
- [3] E.A. Leon-Escamilla, J.D. Corbett, Chem. Mater. 18 (2006) 4782.
- [4] E.A. Leon-Escamilla, J.D. Corbett, J. Solid State Chem. 159 (2001) 149.
- [5] E. A Leon-Escamilla, J.D. Corbett, Inorg. Chem. 40 (2001) 1226.
- [6] W.-M. Hurng, J.D. Corbett, Chem. Mater. 1 (1989) 311.
- [7] S. Gupta, E.A. Leon-Escamilla, F. Wang, G.J. Miller, J.D. Corbett, Inorg. Chem. 48 (2009) 4362.
- [8] Y. Liang, R. Cardoso-Gil, W. Schnelle, M. Schmidt, J.T. Zhao, Y.Z. Grin, Naturforsch. 62b (2007) 935.
- [9] A.C. Larson, R.B. Von Dreele, GSAS: General Structure Analysis System, LANSCE, MS-805, Los Alamos National Laboratory, Los Alamos NM, 1994.
- [10] N. Walker, D. Stuart, Acta Crystallogr. A 39 (1983) 158.
- [11] TEXAN, Single Crystal Structure Analysis Software, Version 5.0, Molecular Structure Corporation, The Woodlands, TX, 1989.
- [12] H.S. Marek, J.D. Corbett, Inorg. Chem. 22 (1983) 3194.
- [13] J.D. Corbett, E. Garcia, A.M. Guloy, W.-M. Hurng, Y.-U. Kwon, E.A. Leon-Escamilla, Chem. Mater. 10 (1998) 2824.
- [14] T.F. Maksudova, P.G. Rustamov, O.M. Oliev, J. Less-Common Met. 109 (1985) L19.